The Effect of β-Turn Structure on the Passive Diffusion of Peptides Across Caco-2 Cell Monolayers

Gregory T. Knipp,[1] David G. Vander Velde,[1] Teruna J. Siahaan,[1] and Ronald T. Borchardt[1,2]

Received April 4, 1997; accepted July 17, 1997

Purpose. To investigate the relationships between the β-turn structure of a peptide and its passive diffusion across Caco-2 cell monolayers, an *in vitro* model of the intestinal mucosa.

Methods. Linear hydrophilic peptides (Ac-TyrProXaaZaaVal-NH_2; Xaa = Gly, Ile and Zaa = Asp, Asn) and hydrophobic (Ac-YaaPro-XaaIleVal-NH_2; Yaa = Tyr, Phe and Xaa = Gly, Ile: and Ac-PhePro-XaaIle-NH_2; Xaa = Gly, Ile) peptides were synthesized and their effective permeability coefficients (P_{eff}) were determined across Caco-2 cell monolayers. The lipophilicities of the peptides were estimated by measuring their partition coefficients ($P_{o/w}$) between 1-octanol and HBSS. Two-dimensional NMR (2D-NMR) spectroscopy and circular dichroism (CD) spectroscopy was used to determine the solution structures of these model peptides.

Results. Using 2D-NMR spectroscopy and CD spectroscopy, the hydrophilic Gly-containing peptides (Ac-TyrProGlyZaaVal-NH_2; Zaa = Asp, Asn) were shown to exhibit a higher degree of β-turn structure in solution than the Ile-containing peptides (Ac-TyrProIleZaaVal-NH_2; Zaa = Asp, Asn). CD spectroscopy was used to show that the Gly-containing hydrophobic peptides (Ac-YaaProGlyIleVal-NH_2; Yaa = Tyr, Phe: and Ac-PheProGlyIle-NH_2) exhibited a higher degree of β-turn structure in solution than the Ile-containing hydrophobic peptides. The P_{eff} values of all four hydrophilic peptides across unperturbed Caco-2 cell monolayers were very low and no statistically significant differences were observed between the Gly- and Ile-containing pentapeptides within either the Asp or Asn series. The P_{eff} values for the hydrophobic Gly-containing peptides were significantly greater than the P_{eff} values determined for their Ile-containing counterparts. The Gly-containing penta- and tetrapeptides in the Phe series, which exhibited high permeation, were shown to be metabolically unstable. In contrast, the Gly- and Ile-containing pentapeptides in the Tyr series and the Ile-containing penta- and tetrapeptides in the Phe series, which exhibited low permeation, were metabolically stable.

Conclusions. Hydrophobic peptides that exhibit significant β-turn structure in solution are more lipophilic as measured by log $P_{o/w}$ and more readily permeate Caco-2 cell monolayers via the transcellular route than hydrophobic peptides that lack this type of solution structure. The ability of these peptides to permeate Caco-2 cell monolayers via the transcellular route also exposed them to metabolism, presumably by cytosolic endopeptidases. Similar secondary structural features in hydrophilic peptides do not appear to sufficiently alter the physicochemical properties of the peptides so as to alter their paracellular flux through unperturbed Caco-2 cell monolayers.

KEY WORDS: peptide delivery; paracellular diffusion; transcellular diffusion; solution conformation; Caco-2 cells.

INTRODUCTION

Natural peptides exhibit extremely low oral bioavailability because of their propensity to be metabolized and their unfavorable physicochemical properties, which largely restrict their permeation across the intestinal mucosa to the paracellular route (1). Since the paracellular route is an aqueous extracellular route, structural features that have been shown to influence the flux of peptides via this pathway include hydrophilicity, charge, and molecular radius (1,2). Recently, Pauletti *et al.* (3) showed that size is the predominant factor in determining the paracellular permeability of peptides having the same charge. In addition, they showed that neutral and positively charged peptides of the same size (e.g., tripeptides) are more permeable than are negatively charged peptides.

However, to achieve optimal permeation of the intestinal mucosa, peptides and peptidomimetics must possess the physicochemical characteristics that allow them to traverse this cellular barrier via the transcellular (or lipid) pathway rather than the paracellular (or aqueous) route (1,2,4). The most important physicochemical characteristics determining transcellular permeation of the intestinal mucosa are size, charge and the components of lipophilicity (i.e., hydrophobicity and hydrogen bonding potential) (4). Another factor that could influence the intestinal mucosal permeation of larger peptides (e.g., pentapeptides) is their conformations in solution. The solution conformation of a peptide could affect various physicochemical characteristics including its size (e.g., molecular radius) and shape (e.g., spherical vs. cylindrical), which might affect its paracellular flux, and/or lipophilicity (e.g., hydrophobicity, hydrogen bonding potential), which might affect its transcellular flux (5).

Recently, our laboratory (5–10) has shown that unique conformations induced by chemical cyclization of peptides can alter these physicochemical parameters (i.e., increased lipophilicity), thus enhancing the overall permeation of the peptide and altering its pathway of permeation from the paracellular to the transcellular pathway. In these cases, the enhanced permeation resulted from an increase in the lipophilicity of the cyclic peptides compared to linear peptides, and thus a shift from a paracellular to a transcellular pathway of flux (5–7). Similar changes in the physicochemical characteristics of linear peptides may result from inducing the peptides to exhibit different types of turn structures in solution (e.g., β-turns, which involve four residues of a peptide where the NH of residue $i + 3$ forms a H-bond with the CO of residue i). The degree to which a peptide exhibits these types of solution structures depends on the amino acid sequence. For example, Dyson *et al.* (11) have shown that the pentapeptides H-TyrProXaaAspVal-OH (Xaa = Gly, Ile) exhibit varying degrees of β-turn structure depending on the Xaa residue (i.e., when Xaa = Gly the peptide exhibits a higher propensity to form β-turn structures in solution than when Xaa = Ile).

[1] Department of Pharmaceutical Chemistry, 2095 Constant Ave., University of Kansas, Lawrence, Kansas 66047.

[2] To whom correspondence should be addressed. (e-mail: Borchardt@smissman.hbc.ukans.edu)

ABBREVIATIONS: TJs, tight junctions; $P_{o/w}$, partition coefficient between 1-octanol and HBSS; P_{eff}, effective permeability coefficient; PC, palmitoyl-DL-carnitine; NMR, nuclear magnetic resonance; CZE, capillary zone electrophoresis; CD, circular dichroism; ACN, acetonitrile; TFA, trifluoroacetic acid; AP, Apical; BL, Basolateral; HBSS, Hanks' balanced salt solution; HOHAHA, Homonuclear Hartmann Hahn spectroscopy; ROESY, rotating frame Overhauser spectroscopy; DSS, 2,2-dimethyl-2-silapentane-5-sulfonate.

0724-8741/97/1000-1332$12.50/0

To our knowledge, no attempts have been made to determine how these types of turn structures in linear peptides influence their paracellular and transcellular permeation across cell monolayers. In the present study, we have designed experiments to investigate whether β-turn structures in solution can influence the permeability of a linear peptide across the Caco-2 cell monolayers. For these studies, we have used five pairs of model penta- and tetra-peptides. Since H-TyrProXaaAspVal-OH (Xaa = Gly, Ile) are metabolically unstable, we prepared the N-terminally acetylated and C-terminally amidated analogs (Ac-TyrProXaaAspVal-NH_2, Xaa = Gly, Ile) to block metabolism by exopeptidases. We also prepared the Asn analogs (Ac-Tyr-ProXaaAsnVal-NH_2, Xaa = Gly, Ile) of these pentapeptides to determine the effect of charge on the paracellular permeation. In addition, maintaining the ProGly and ProIle motifs as determinants for β-turn structure, we varied the amino acid sequence on the N-terminal end (i.e., Tyr replaced with Phe) and the C-terminal end (i.e., AspVal replaced by IleVal or Ile) in order to increase their hydrophobicity. Thus, the resulting model pentapeptides (Ac-ZaaProXaaIleVal-NH_2; Zaa = Tyr, Phe and Xaa = Gly, Ile) and tetrapeptides (i.e., Ac-PheProXaaIle-NH_2; Xaa = Gly, Ile) should have a greater propensity to traverse Caco-2 cell monolayers by the transcellular pathway than by the paracellular pathway.

MATERIALS AND METHODS

Materials

[^{14}C]Mannitol (specific activity = 55 μCi/μmol) was purchased from American Radiolabeled Company (St. Louis, MO). Palmitoyl-DL-carnitine (PC) was purchased from Sigma Chemical Company (St. Louis, MO). Hanks' balanced salt solution (HBSS) was purchased from JRH Biosciences (Lenexa, KS). All the amino acids, in the L-configuration where applicable, and resins used for the solid-phase synthesis of the peptides were purchased from Bachem Bioscience Inc. (King of Prussia, PA). [^{14}C]Ac-Phe-NH_2 (specific activity = 100 μCi/μmol) was generously provided by Dr. Philip Burton of Pharmacia & Upjohn Inc. (Kalamazoo, MI).

Peptide Synthesis

The N- and C-terminally capped peptides were synthesized using solid-phase methodology and 9-fluorenylmethoxycarbamate (FMOC)-protected amino acids on a 4-(2′,4′-dimethoxyphenyl-FMOC-aminomethyl)-phenoxymethyl polystyrene resin as described previously (10). All of the amino acids, except Pro, Tyr, and Phe, were added to the peptide on the resin at a 2.5 molar excess and allowed to couple for 2 hr. Pro, Tyr, and Phe were coupled three times at a 1:1 molar ratio. The first two couplings were performed for 2 hr, followed by an overnight coupling. Coupling was confirmed by the Kaiser test. The crude peptide mixtures were purified by gradient elution HPLC using a Whatman preparative C18 column (21.4 mm × 25 cm). The eluents for the hydrophilic peptides consisted of Milli-Q H_2O:acetonitrile (ACN):trifluoroacetic acid (TFA) in ratios of 95:5:0.1 (solvent A) and 20:80:0.1 (solvent B). Gradient elution was performed with a 5 mL/min flow rate and a gradient increase of 5–50% of solvent B over 40 min. The eluents for the hydrophobic peptides consisted of Milli-Q H_2O:ACN:TFA in ratios of 80:20:0.1 (solvent A) and 10:90:0.1 (solvent B). Gradient elution was performed with a 5 mL/min flow rate. The gradient conditions consisted of an increase of 5–50% of solvent B over 30 min, followed by a increase of 50–100% of solvent B over the next 30 min; the gradient was then held at 100% of solvent B for 20 min. The fractions containing peptide were identified by mass spectroscopy and purity was assured by analytical HPLC. All solvents were HPLC grade or better.

NMR Spectroscopy

The NMR experiments were performed on the hydrophilic peptides (Ac-TyrProXaaZaaVal-NH_2; Xaa = Gly, Ile and Zaa = Asp, Asn) at 10°C in 90% H_2O/10% D_2O with the pH adjusted to 4.1 ± 0.1 using 0.1 N NaOH and 0.1 N HCL. 2,2-Dimethyl-2-silapentane-5-sulfonate (DSS) was added as a chemical shift standard. The peptide concentrations typically ranged from 25 to 35 mM in 0.6 mL of the solvent. All experiments were performed on a Brüker AM-500 spectrometer operating at 500.138 MHz for ^{1}H and using a dedicated proton probe that was modified for optimal suppression of the unwanted water resonance. Phase-sensitive Homonuclear Hartmann Hahn (HOHAHA) and rotating frame Overhauser (ROESY) spectra were taken as described previously (7,10). The data were processed with a squared cosine bell apodization in both dimensions; the f1 axis was zero filled to 1 K points for the HOHAHA and 2 K points for the ROESY.

The amide temperature coefficients for the peptides were obtained from one-dimensional spectra using the ^{1}H presaturation program on the Brüker AM-500 spectrometer. The amide proton chemical shifts (ppm) were measured over a range of 10–35°C. The amide temperature coefficients were calculated from the slopes of the plots of the Δppm for each amide proton vs. temperature.

CD Spectroscopy

The CD spectra for the peptides were determined at 25°C on an Aviv 62 DS spectropolarimeter (Lakewood, NJ) as described previously (7,10). The peptide concentrations for these studies ranged from 1–2 mM in methanol. The spectra were deconvoluted using the convex constraint analysis method and secondary structural elements were estimated as described previously (7,10).

Molecular Size Determinations

CZE was used to determine aqueous diffusion coefficients in HBSS by a stop-flow method described by Yao and Li (12). The analysis was performed at 37°C on an ISCO model 3140 capillary electropherogram instrument. The voltage applied across the capillary was 10 kV, which led to a current of approximately 55 μA. The capillary used was uncoated and measured 40 cm from the buffer reservoir to the detector. The molecular radius (r) for each peptide was calculated from its diffusion coefficient (D) by the Stokes-Einstein equation:

$$r = \frac{kT}{6\pi\eta D} \quad (1)$$

where kT = thermal energy and η = viscosity.

Partition Coefficient Determinations

The lipophilicities of the hydrophilic (Ac-TyrProXaaZaa-Val-NH_2; Xaa = Gly, Ile and Zaa = Asp, Asn) and hydrophobic (Ac-YaaProXaaIleVal-NH_2; Yaa = Tyr, Phe and Xaa = Gly, Ile: and Ac-PheProXaaIle-NH_2; Xaa = Gly, Ile) peptides were estimated by measuring the partition coefficients ($P_{o/w}$) of these molecules in 1-octanol and HBSS. $P_{o/w}$ values for the hydrophilic peptides were determined in triplicate at volume ratios of 25:1, 35:1, and 45:1 (octanol:HBSS). $P_{o/w}$ values for Ac-TyrProXaaIleVal-NH_2 (Xaa = Gly, Ile) were determined in triplicate at volume ratios of 5:1, 2:1, and 1:1 (octanol:HBSS). $P_{o/w}$ values for each Phe-containing peptide were determined in triplicate at volume ratios of 1:1, 1:2, and 1:5 (octanol:HBSS). The concentration of the peptides in HBSS ranged from about 1–2 mM. The concentration of the peptides in HBSS ranged from about 1–2 mM. All equilibration steps were performed by vigorously shaking the two phases together for 24 hr. The samples were then centrifuged to facilitate phase separation. The concentration in the aqueous phase (Ca) was then determined by HPLC as described below. All but 5 mL of the organic phase in each sample was then transferred to a separate tube and re-equilibrated with 1 mL of HBSS to assess the concentration of peptide in the organic phase (Co). The partition coefficients were calculated by Equation 2:

$$P_{o/w} = \left(\frac{Co}{Ca}\right) \times \left(\frac{Va}{Vo}\right) \quad (2)$$

where Va and Vo are the volumes of the aqueous and organic phases, respectively.

Cell Culture

The Caco-2 cell line, which originated from a human adenocarcinoma (13), was obtained from the American Type Culture Collection (Rockville, MD). The conditions under which the cells were grown have been described previously by our laboratory (14). The cells used in this study were between passages 35 and 70. Mannitol fluxes were monitored in triplicate across unperturbed cell monolayers to determine monolayer integrity. All cell monolayers used in these studies, irrespective of passage number, exhibited mannitol fluxes < 0.4% per hr.

Caco-2 Transport Experiments

The Caco-2 transport experiments were conducted as described previously by our laboratory (3,5,6,10) with a few modifications. Caco-2 transport studies with [^{14}C]mannitol and [^{14}C]Ac-Phe-NH_2 were conducted following the same procedure for radiolabeled solutes described previously (14). For transport experiments performed in the presence of PC, the cells were incubated with the appropriate concentrations of PC in HBSS on both the apical (AP) and basolateral (BL) sides. The peptides were prepared as stock solutions at concentrations of 0.4–0.7 mM in HBSS, or in HBSS containing PC. Sampling for the Gly- and Ile-containing peptides in the Tyr series and the Ile-containing tetra- and pentapeptides in the Phe series was performed as described previously (3,5,10). Due to increased permeation and metabolism, the receiver side sampling of the Gly-containing tetra- and pentapeptides in the Phe series was reduced from every 30 min over 3 hr to every 5 min over 50 min. Samples were stored in the freezer (−20°C) until analyzed. No degradation was observed during this storage period. The effective permeability coefficients (P_{eff}) for all of the transport experiments were calculated from the appearance kinetics of the solute in the receiver compartment at steady state as described previously (14). A one-way ANOVA($r > 95\%$) with a Tukey's comparison was performed to compare the observed P_{eff} values.

HPLC Analysis

The peptide transport samples were analyzed by gradient reversed-phase HPLC on a Rainin Dynamax 300A C18 column (5 mm, 4.6 × 250 mm) with a Dynamax C18 guard column. The eluents for the hydrophilic Tyr-containing peptides Ac-TyrProXaaZaaVal-NH_2 (Xaa = Gly, Ile and Zaa = Asp, Asn) consisted of Milli-Q H_2O:ACN:TFA in ratios of 95:5:0.1 (solvent A) and 20:80:0.1 (solvent B). Elution was accomplished using a gradient that consisted of ramping from 0–30% B over 15 minutes. The eluents for the analysis of the (Ac-TyrProXaaIleVal-NH_2; Xaa = Gly, Ile) consisted of Milli-Q H_2O:ACN:TFA in ratios of 90:10:0.1 (solvent A) and 20:80:0.1 (solvent B). Elution was accomplished using a gradient that consisted of ramping from 0–30% B over 12 min. The eluents for the analysis of the hydrophobic Phe-containing peptides (Ac-PheProXaaIleVal-NH_2; Xaa = Gly, Ile and Ac-PheProXaaIle-NH_2; Xaa = Gly, Ile) consisted of Milli-Q H_2O:ACN:TFA in ratios of 75:25:0.1 (solvent A) and 20:80:0.1 (solvent B). Elution was accomplished using a gradient that consisted of ramping from 10–45% B over 10 min, then ramping from 45–90% from 10–15 min. The fluorescence detector was set to excitation and emission wavelengths of 278 and 305 nm, respectively, for the Tyr-containing peptides and 257 and 282 nm, respectively, for the Phe-containing peptides. A flow rate of 1.0 mL/min was used.

RESULTS

The Physicochemical Properties

The physicochemical properties of the model peptides are shown in Table I. The 1-octanol:HBSS log $P_{o/w}$ values for the hydrophilic peptides (Ac-TyrProXaaZaaVal-NH_2; Xaa = Gly, Ile and Zaa = Asp, Asn) were negative, confirming their hydrophilic characteristics. Two trends become apparent upon analysis of the partitioning behavior of these peptides: (a) the Asp analogs are more hydrophilic than the Asn analogs; and (b) the Gly-containing analogs are more hydrophilic than the Ile-containing analogs in each series. For the hydrophobic peptides, the 1-octanol:HBSS log $P_{o/w}$ value for Ac-TyrProGlyIleVal-NH_2 was positive and higher than the log $P_{o/w}$ value for the Ac-TyrProIleIleVal-NH_2. The 1-octanol:HBSS log $P_{o/w}$ values for the peptides in the Phe series were all positive. Two trends become apparent upon analysis of the partitioning behavior of the peptides in the Phe series: (a) the Gly analogs were more hydrophobic than the Ile analogs; and (b) the partitioning characteristics of the Gly- and Ile-containing pentapeptides were similar to those of the tetrapeptides in the Phe series.

The diffusion coefficients, which were determined by CZE, were used to calculate the molecular radii by the Stokes-Einstein equation. For the hydrophilic peptides, the molecular radii of the Asn-containing peptides were consistently smaller than the

Table I. Physicochemical Properties of the Model Peptides

Peptide	Molecular weight	Diffusion coefficient[a] ($\times 10^6$ cm^2/s)	Molecular radius (Å)[b]	Log $P_{o/w}$[c]	Net charge
Ac-TyrProIleAspVal-NH_2	646	5.7	5.8	−1.85	Negative
Ac-TyrProGlyAspVal-NH_2	590	5.1	6.5	−3.71	Negative
Ac-TyrProIleAsnVal-NH_2	645	6.5	4.7	−0.42	Neutral
Ac-TyrProGlyAsnVal-NH_2	589	7.5	4.4	−2.06	Neutral
Ac-TyrProIleIleVal-NH_2	644	5.7	5.7	1.13	Neutral
Ac-TyrProGlyIleVal-NH_2	588	7.2	4.8	−0.20	Neutral
Ac-PheProIleIleVal-NH_2	628	6.2	5.4	1.61	Neutral
Ac-PheProGlyIleVal-NH_2	572	6.4	5.1	1.96	Neutral
Ac-PheProIleIle-NH_2	529	6.1	5.4	1.17	Neutral
Ac-PheProGlyIle-NH_2	473	7.3	4.5	2.00	Neutral

[a] Diffusion coefficients were determined by stop-flow capillary electrophoresis in HBSS at pH 7.35.
[b] The molecular radius was calculated from the diffusion coefficient by the Stokes-Einstein equation.
[c] The partition coefficients were determined in 1-octanol:HBSS as described in Materials and Methods.

molecular radii of the Asp-containing peptides. However, there were no consistent differences between the molecular radii of the Gly- and Ile-containing peptides within either the Asp or Asn series. For the hydrophobic Tyr- and Phe-containing peptides, the molecular radius of the Gly-containing peptide within each pair was consistently smaller than the molecular radius of its Ile-containing counterpart.

To confirm that the N-terminally acetylated and C-terminally amidated pentapeptides (Ac-TyrProXaaZaaVal-NH_2; Xaa = Gly, Ile and Zaa = Asp, Asn) used as models in this study had solution conformations similar to those described by Dyson *et al.* (11) for H-TyrProXaaAspVal-OH_2 (Xaa = Gly, Ile), extensive 2D-NMR and CD experiments were conducted. Unambiguous assignments of the sequence specific proton chemical shifts were obtained for each residue from the HOHAHA spectrum of each peptide. The chemical shifts (NH, $C^{\alpha}H$, and $C^{\beta}H$), the coupling constants between the amide and α protons [$^3J_{HN\alpha H}$ (Hz)], and the amide temperature coefficients for Ac-TyrProGlyAsnVal-NH_2 are shown in Table II. All of the amide-α coupling constants for each residue were greater than 5.

Unambiguous assignment of the sequence-specific through-space connectivities was obtained from the ROESY spectrum of each peptide. For example, in Ac-TyrProGlyAsnVal-NH_2, the NH of Asn4 has a through-space ROE connectivity with the NH of Gly3 (d_{NN}) and the Pro2 δH has a through-space ROE connectivity with the Gly3 NH ($d_{N\delta}$). These ROE connectivities have been shown to be associated with a 4 → 1 Type I β-turn (Figure 1) (11). This conclusion is supported by the relatively reduced amide temperature coefficient found for the Asn4 NH (−6.3 ppb/K as compared to ≈ −11 ppb/K for free amide protons), indicating that it forms an intramolecular hydrogen bond with the carbonyl of Tyr1. Interestingly, evidence was also found for the presence of a 5 → 2 Type I β-turn as shown in Figure 1. A d_{NN} ROE connectivity replaces the $d_{N\delta}$ when Pro is replaced in the turn by any other residue. Evidence for this 5 → 2 Type I β-turn includes a d_{NN} connectivity between Gly3 and Asn4, a d_{NN} connectivity between Asn4 and Val5, and a $d_{N\alpha}$ between Val5 and Gly3, The NMR spectral data for H-TyrProGlyAspVal-OH and Ac-TyrProGlyAspVal-NH_2 were found to be similar to the data described above for Ac-TyrProGlyAsnVal-NH_2 (data not shown). The ROE connectivities observed for H-TyrProIleAspVal-OH, Ac-TyrProIleAspVal-NH_2, and Ac-TyrProIleAsnVal-NH_2 indicated that these peptides lack similar β-turn conformations in solution (data not shown). Due to technical difficulties, the NMR spectra for the remaining peptides were not obtained. Instead, CD spectroscopy was used to determine their solution structures.

Table II. Temperature Coefficients, Coupling Constants, and Chemical Shift Data for Ac-TyrProGlyAsnVal-NH_2 in 90% H_2O and 10% D_2O

Residue	Δδ/ΔT [ppb/K]	Coupling constant $^3J_{HN\alpha H}$(Hz)	Chemical shift in (ppm) NH	$C^{\alpha}H$	$C^{\beta}H$
Tyr1	−9.3	7.30	8.21	4.73	2.98, 2.76
Pro2	NA	NA	NA	4.38	2.22, 2.01
Gly3	−8.7	6.38[a]	7.96	3.82	NA
Asn4	−6.3	6.67	8.27	4.63	2.63
Val5	−8.9	7.45	8.18	3.95	2.14

NA-not applicable.
[a] For Gly, the coupling constant is $^3J_{HN\alpha H2}$ (Hz).

The CD spectra for Ac-TyrProGlyAsnVal-NH_2 and Ac-TyrProIleAsnVal-NH_2 are shown in Figure 2. The CD spectrum for the Gly-containing pentapeptide shows a minimum at 220 nm, which has been shown to be characteristic of a Type I β-turn (7,15). The CD spectrum for Ac-TyrProIleAsnVal-NH_2 lacks this feature. Upon deconvolution of the spectra for the Asn peptides, it was apparent that the Gly-containing peptide has a significantly higher population of β-turn structure in solution than the Ile-containing peptide (data not shown). Similar results were found for all of the other peptide pairs used in these studies (data not shown).

Transport Studies Across Caco-2 Cell Monolayers

In preliminary experiments, attempts were made to determine the permeability characteristics of the uncapped pentapeptides (i.e., H-TyrProXaaAspVal-OH: Xaa = Gly, Ile). However, because of their rapid metabolism when applied to the AP side of the Caco-2 cell monolayer, the uncapped peptides were not

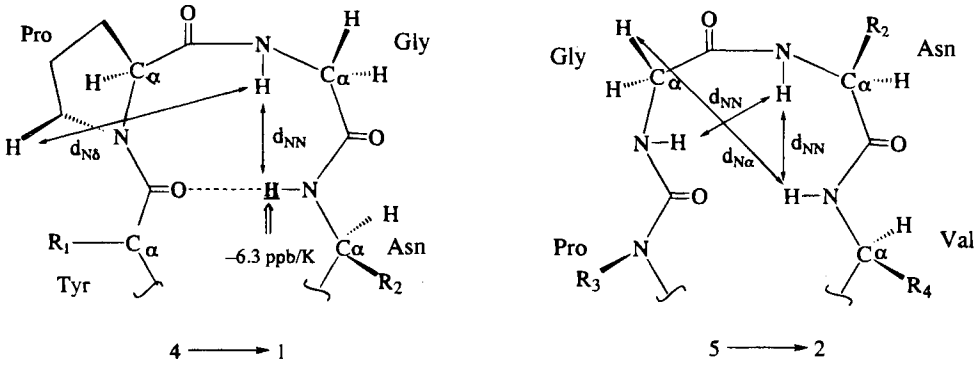

Fig. 1. The ROE connectivities that support the presence of 4 → 1 Type I and 5 → 2 Type I β-turns in Ac-TyrProGlyAsnVal-NH_2.

detected on the BL side even after a 3 hr incubation (data not shown). Based on the limits of detection of the HPLC assay, the maximum P_{eff} values of the uncapped analogs were estimated to be $\approx 3 \times 10^{-9}$ cm/s.

When the N- and C-terminally capped hydrophilic peptides (Ac-TyrProXaaZaaVal-NH_2; Xaa = Gly, Ile and Zaa = Asp, Asn) were applied to the AP side of the Caco-2 cell monolayers, they were metabolically stable for up to 3 hr (data not shown). In addition, detectable amounts were measured on the BL side of the monolayer, allowing for the estimation of P_{eff} values for each pentapeptide. The data shown in Table III suggest that both the Gly- and Ile-containing Asn peptides exhibit slightly higher P_{eff} values than their corresponding Asp analogs; however, the differences were not statistically significant. In addition, within each series, the Ile-containing peptide appears to be more permeable than the Gly-containing peptide; however, again the differences were not statistically significant.

To confirm that the hydrophilic pentapeptides traverse the Caco-2 cell monolayer via the paracellular route, the monolayers were perturbed with PC to increase the aqueous pore radius from approximately 5.1 Å to 12 Å (14). For comparison purposes, experiments were also performed with [^{14}C]mannitol, a known paracellular marker (13,16), and [^{14}C]Ac-Phe-NH_2, a known transcellular marker (17). As shown in Table III, the P_{eff} value of [^{14}C]mannitol in the PC-perturbed Caco-2 cell monolayer is approximately 33 times greater than the P_{eff} value in unperturbed monolayers. In comparison, the P_{eff} value of [^{14}C]Ac-Phe-NH_2 increases only 2.7 times in the PC-perturbed monolayer system as compared to the unperturbed system.

When the P_{eff} values of the model hydrophilic pentapeptides were determined in the PC-perturbed Caco-2 cell monolayer system, they were shown to be 130–350 times greater than the P_{eff} values determined in the unperturbed Caco-2 cell monolayer system (Table III). It is interesting to note that in the PC-perturbed monolayer system, the Asp-containing pentapeptides exhibited lower P_{eff} values than their counterparts in the Asn series. In addition, the Gly-containing Asn pentapeptide exhibited a higher P_{eff} value than the Ile-containing Asn pentapeptide. A similar difference was not observed between the permeability characteristics of the Gly- and Ile-containing peptides in the Asp series.

When the hydrophobic peptides Ac-TyrProGlyIleVal-NH_2, Ac-TyrProIleIleVal-NH_2, Ac-PheProIleIleVal-NH_2 and Ac-PheProIleIle-NH_2 were applied to the AP side of the Caco-2 cell monolayers, they were shown to be metabolically stable for up to 3 hr (data not shown). In contrast, Ac-PheProGly-

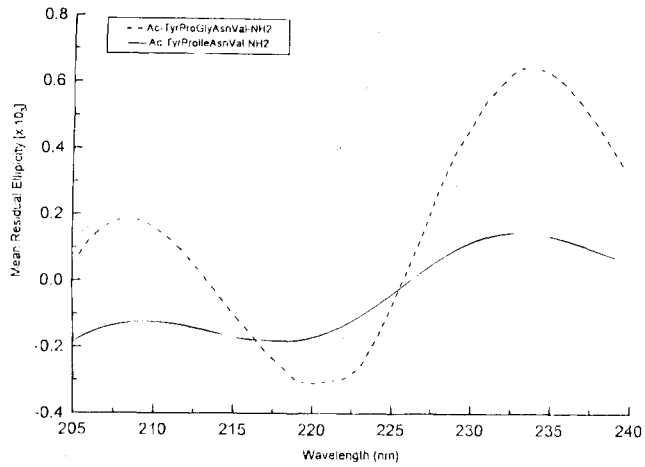

Fig. 2. The CD spectra for Ac-TyrProGlyAsnVal-NH_2 and Ac-TyrProIleAsnVal-NH_2.

Table III. Observed P_{eff} Values of the Hydrophilic Pentapeptides Across Unperturbed and Perturbed Caco-2 Cell Monolayers

Compound	P_{eff} ($\times 10^6$ cm/s)[a]		Relative increase[d]
	Unperturbed[b]	Perturbed[c]	
Mannitol	0.237 (0.01)	7.94 (0.88)	33.5
Ac-Phe-NH_2	9.31 (0.28)	25.2 (5.23)	2.7
Ac-TyrProGlyAspVal-NH_2	0.050 (0.010)	6.81 (0.81)	136
Ac-TyrProIleAspVal-NH_2	0.083 (0.017)	10.9 (1.45)	131
Ac-TyrProGlyAsnVal-NH_2	0.084 (0.021)	29.7 (0.60)	353
Ac-TyrProIleAsnVal-NH_2	0.097 (0.017)	16.5 (0.44)	170

[a] Permeability coefficients are expressed as the mean ± (s.d.) for n = 3.
[b] Determined using Caco-2 cell monolayers grown onto microporous membranes as described in Materials and Methods.
[c] Determined using Caco-2 cell monolayers grown onto microporous membranes and then perturbed by incubation with 0.15 mM PC as described in Materials and Methods.
[d] Ratio of P_{eff} (perturbed)/P_{eff} (unperturbed).

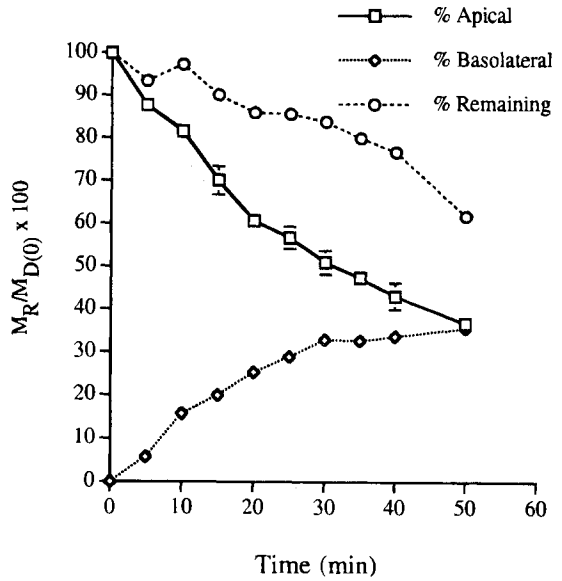

Fig. 3. The time course for transport and the stability of Ac-PheProGly-IleVal-NH_2 after application of the peptide on the AP side of Caco-2 cell monolayers. The values for % Remaining were calculated by adding the % Apical and % Basolateral sides together at each time point.

IleVal-NH_2 and Ac-PheProGlyIle-NH_2 were found to undergo rapid metabolism when applied to the AP side of the Caco-2 cell monolayers (Figure 3). Therefore, the P_{eff} values of these peptides had to be calculated from the initial rates of the appearance kinetics on the receiver side. The data shown in Table IV suggest that the Gly-containing peptides exhibit significantly higher P_{eff} values than their corresponding Ile analogs in all three pairs of peptides. In addition, replacement of a Tyr residue with a Phe residue significantly increases the permeation of both the Gly- and Ile-containing peptides.

DISCUSSION

Recently, our laboratory has shown that restricting the conformation of a hexapeptide by different cyclization methods enhances its permeation across Caco-2 cell monolayers (5–10). The enhanced permeation appears to result from changes in the physicochemical characteristics (i.e., lipophilicity) of the cyclic peptides compared to the linear peptide, which cause a shift from a paracellular to a transcellular pathway of flux (5,6,10). Based on these observations with cyclic peptides, we hypothesized that the solution conformation (i.e., β-turn) of a linear peptide may also influence its physicochemical characteristics and, thus, its permeation across Caco-2 cell monolayers. A series of model hydrophilic peptides (Ac-TyrProXaaZaaVal-NH_2; Xaa = Gly, Ile and Zaa = Asp, Asn) and hydrophobic peptides (Ac-YaaProXaaIleVal-NH_2; Yaa = Tyr, Phe and Xaa = Gly, Ile: and Ac-PheProXaaIle-NH_2; Xaa = Gly, Ile) were designed to investigate the relationship between the β-turn structure of peptides, their physicochemical characteristics, and their permeation across Caco-2 cell monolayers. Each series contained a peptide with the ProGly motif and a peptide with the ProIle motif as determinants of β-turn structure. Since this series of peptides varies significantly in lipophilicity, as measured by their log $P_{o/w}$ in 1-octanol and HBSS, they should permeate the Caco-2 cell monolayers by the paracellular and/or transcellular routes.

Initially, extensive 2D-NMR and CD spectroscopy studies were conducted to determine the population of β-turn structure in these hydrophilic peptides. As pointed out by Dyson *et al.* (11), ROE connectivities from 2D-NMR ROESY spectra can be used to identify even small amounts of β-turn structures in dynamic equilibrium with random coil forms within this class of peptides. The ROE connectivities observed for Ac-TyrPro-XaaAspVal-NH_2 and Ac-TyrProXaaAsnVal-NH_2 (Xaa = Gly, Ile) are consistent with the findings reported by Dyson *et al.* (11) for the uncapped H-TyrProXaaAspVal-OH (Xaa = Gly, Ile) peptides. These findings suggest that the Gly-containing peptides exist in dynamic equilibrium between a 4 → 1 Type I β-turn and a 5 → 2 Type I β-turn. The ROESY spectra for the Ile-containing peptides did not exhibit the same degree or intensity of connectivities (data not shown), suggesting these peptides exist in random conformations.

The presence of Type I β-turns in the Gly-containing peptides was also strongly supported by the CD spectra (i.e., Ac-TyrProGlyAsnVal-NH_2, Figure 2) (7,15). The CD spectra for the Ile-containing peptides (i.e., Ac-TyrProIleAsnVal-NH_2, Figure 2) suggested a more random structure for these peptides (15). The results of these experiments clearly showed that CD could be used to determine the relative degree of β-turn structure that these peptide pairs exhibit, as illustrated in Figure 2. The CD spectra for the remaining peptide pairs clearly showed that all of the peptides containing the ProGly motif exhibit significant β-turn structure in solution, whereas the analogous peptide in each pair containing the ProIle motif lack this structural feature (data not shown). These results are consistent with the findings of Dyson *et al.* (11).

The very low P_{eff} values determined for the hydrophilic peptides using unperturbed Caco-2 cell monolayers are similar to values observed for a series of N-terminally and C-terminally blocked hexapeptides (3). The similarities in the permeation characteristics of these model penta- and hexapeptides include the observation that the negatively charged peptides appear to be slightly less (but not statistically significant) less able to permeate than the neutral peptides, which is consistent with the charge characteristics of the TJs in Caco-2 cell monolayers (14,16). The very low P_{eff} values also suggest that these peptides exhibit predominantly paracellular flux across Caco-2 cell monolayers.

In an attempt to determine the effect of the size and/or shape of these hydrophilic peptides on their permeation of the Caco-2 cell monolayers, the permeability characteristics of the

Table IV. Observed P_{eff} Values of the Hydrophobic Penta- and Tetrapeptides Across Caco-2 Cell Monolayers

Peptides	P_{eff} ($\times 10^6$ cm/s)[a,b]
Ac-TyrProIleIleVal-NH_2	0.05 ± (0.01)
Ac-TyrProGlyIleVal-NH_2	0.34 ± (0.14)
Ac-PheProIleIleVal-NH_2	0.47 ± (0.27)
Ac-PheProGlyIleVal-NH_2	58.7 ± (1.1)
Ac-PheProIleIle-NH_2	0.45 ± (0.11)
Ac-PheProGlyIle-NH_2	59.1 ± (2.4)

[a] Permeability coefficients are expressed as the mean ± s.d. for n = 3.
[b] Determined using Caco-2 cell monolayers grown onto microporous membranes as described in Materials and Methods.

Gly-containing hydrophilic peptides were compared to Ile-containing peptides. Interestingly, the Ile-containing peptides in both the Asp and Asn series were slightly more able to permeate across the unperturbed Caco-2 cell monolayer than were the Gly-containing peptides. These results do not suggest a role for the β-turn structure in determining permeation of these peptides via the paracellular route in unperturbed Caco-2 cell monolayers.

In earlier studies, our laboratory (14) has shown that the average size of the aqueous pores in the TJs of the Caco-2 cell monolayers is approximately 5.1 Å. From the data shown in Table I, it is apparent that the pentapeptides used in this study have molecular radii (range 4.4–6.5 Å) in the same size range as the pores in the cellular TJs. Therefore, it is not surprising that these model pentapeptides exhibit extremely low permeation across Caco-2 cell monolayers and that slight changes in solution conformation induced by β-turn structures may not significantly affect their P_{eff} values.

To confirm that the hydrophilic peptides used in this study are permeating the Caco-2 cell monolayers predominantly by the paracellular route, transport experiments were conducted using Caco-2 cell monolayers that had their TJs slightly perturbed by PC. A similar strategy has been employed by Artursson and Magnusson (18) and Gan *et al.* (19) using EGTA as a perturbant. For these studies, PC was employed because our laboratory had shown previously that this perturbant increased the aqueous pore radii of the TJs in Caco-2 cell monolayers in a dose-dependent manner (14). A concentration of 0.15 mM PC was selected, which increased the aqueous pore radius from approximately 5.1 Å to approximately 12 Å (14).

From the data shown in Table III, it is apparent that the hydrophilic peptides exhibit significantly higher P_{eff} values in the PC-perturbed Caco-2 cell monolayers than in unperturbed cell monolayers (i.e., 131–136 fold for the Asp peptides and 170–353 fold for the Asn peptides). These results are consistent with the data observed for mannitol, a known marker of the paracellular pathway (14,16) (i.e., 33.5 fold increase in the P_{eff} value in perturbed vs. unperturbed cell monolayers) but not consistent with data for Ac-Phe-NH_2, a known marker of the transcellular route (17) (i.e., 2.7 fold increase in the P_{eff} value in perturbed vs. unperturbed cell monolayers). These observations further confirm that these peptides traverse the Caco-2 cell monolayers predominantly by the paracellular pathway. Interestingly, the rank order of the P_{eff} values of these pentapeptides across perturbed Caco-2 cell monolayers is consistent with their molecular radii, which would be predicted by the Renkin molecular sieving function (14,16).

In comparing the Asp- and Asn-containing peptides, it is also apparent that the P_{eff} values of the negatively charged Asp peptides are significantly lower across the PC-perturbed Caco-2 cell monolayers than the P_{eff} values for the neutral Asn peptides. These observations are consistent with data published earlier by our laboratory (3) using a series of hexapeptides. Both the results reported in this paper and our earlier work (3) show that there is an effect of charge on the paracellular permeation of these peptides (i.e., anionic peptides exhibit a reduced flux as compared to the neutral or cationic peptides of similar size and structure). When a comparison was made between the P_{eff} values of the Gly- and Ile-containing pentapeptides in the Asp series determined in the PC-perturbed Caco-2 cell monolayers, no statistically significant difference was observed, suggesting that the negative charge on these peptides may be the predominant factor in controlling their paracellular permeation.

In the case of the Asn series, a statistically significant difference was found in the P_{eff} values of the Gly- and Ile-containing peptides (i.e., the Gly-containing peptide has a two-fold higher P_{eff} value than the Ile-containing peptide). Therefore, with this series of neutral pentapeptides, solution conformation appears to affect the size and/or shape of the molecule sufficiently to influence its permeation of the cell monolayer via the paracellular route.

Except for Ac-TyrProGlyIleVal-NH_2, all of the hydrophobic peptides exhibited positive log $P_{o/w}$ values suggesting that they should more readily permeate the Caco-2 cell monolayers via the transcellular route. It is interesting to note that in the Tyr series of pentapeptides, the Gly-containing peptides have lower log $P_{o/w}$ values than the Ile-containing peptides, which is consistent with partitioning behavior of the hydrophilic peptides. However, when the Tyr residue in these hydrophobic pentapeptides is replaced with a Phe residue, this trend is reversed (i.e., the Gly-containing peptide has a higher log $P_{o/w}$ value than the Ile-containing peptide). This observation suggests that, in the Phe series of pentapeptides, the presence of β-turn structure in the Gly-containing peptide contributes significant lipophilic character to the peptide. This would not be expected when one considers that the hydrophobic contribution from an Ile residue is much greater than that of a Gly residue (20). Similar partitioning behavior between 1-octanol and HBSS was observed for the Phe series of tetrapeptides (Table I). It should be noted that attempts were made to measure the hydrogen bonding potential of all three series of peptides; however, technical difficulties were encountered in measuring partition coefficients in the *iso*-octane:HBSS system.

The Asn residue of the hydrophilic peptides, as mentioned above, was replaced by an Ile residue in these hydrophobic peptides (i.e., Ac-TyrProXaaIleVal-NH_2; Xaa = Gly, Ile) in an attempt to increase the hydrophobicity (20). The low P_{eff} value (5×10^{-8} cm/s) determined for the Ile-containing peptide in this series suggests that it also permeates the Caco-2 cell monolayers predominantly by the paracellular route. However, it is interesting to note that the Gly-containing peptide in this series showed a P_{eff} value (34×10^{-8} cm/s) that was approximately 8 times higher than that of the Ile-containing peptide, suggesting the possibility that this peptide because of its solution structure may have a significant transcellular component to its permeation across Caco-2 cell monolayers.

In an attempt to further increase the hydrophobicity of these pentapeptides, we replaced the Tyr residue with a Phe residue (i.e., Ac-PheProXaaIleVal-NH_2; Xaa = Gly, Ile). This structural change was made based on the observation by Burton *et al.* (21) that the permeation of a D-Phe dipeptide was almost an order of magnitude higher than that of the D-Tyr dipeptide. Consistent with the observations made by Burton *et al.* (21), replacement of the Tyr residue by a Phe residue in our model pentapeptides resulted in a significant increase in the Caco-2 cell permeability of these peptides. For example, in the case the Ile-containing pentapeptide in the Phe series, the P_{eff} value was approximately an order of magnitude greater than the P_{eff} value observed for its counterpart in the Tyr series. In the case of the Gly-containing pentapeptides, the peptide in the Phe series was approximately 170 times more able to permeate than was the peptide in the Tyr series.

When comparisons were made between the P_{eff} values of the Gly-containing and Ile-containing pentapeptides in the Phe series, dramatic differences were observed (Table IV). Consistent with the partitioning characteristics of these peptides (Table I), the Gly-containing peptide (Ac-PheProGlyIleVal-NH_2) was shown to be approximately 125 times more able to permeate than the Ile-containing peptide (Ac-PheProIleIleVal-NH_2). This relatively high permeation for a peptide suggests that its β-turn structure has a significant influence on its ability to partition into a lipid bilayer and traverse the monolayer by the transcellular pathway.

The effect of solution conformation (β-turn structures) on transcellular permeation of biological membranes may be readily understood from the effect membranes have been shown to exert on the solution conformation of linear peptides. For example, the membrane interface has been shown to induce the formation of a β-turn in linear peptides that exhibit random solution conformations (22,23). Two-dimensional NMR studies with Ac-LysGlyArgGlyAspGly-NH_2 showed that the conformation of the peptide was highly random in solution and in the presence of deuterated dodecyl-phosphocholine micelles (22). This peptide was then covalently anchored to 2,3-dipalmitoyl-D-(+)-glyceric acid through the Lys side chain to form a lipopeptide, which also did not alter the random structure of the peptide in solution. However, when the solution structure of this lipopeptide was determined in deuterated dodecyl-phosphocholine, which forms micelles, the peptide was shown to adopt a Type (II/I′) β-turn conformation (22). A similar phenomenon was also witnessed with membrane-bound conformations of Leu-enkephalin analogs (23). These results suggest that unique solution conformations can be induced in peptides as they approach a membrane interface, which may be an important step in the transcellular permeation of peptides. The possibility that solution conformation may influence the transcellular permeation of peptides has also been discussed by Burton *et al.* (4).

In an attempt to further increase the hydrophobicity of peptides in the Phe series, we truncated the pentapeptides by removal of the Val residue on the C-terminal end to make a series of tetrapeptides (i.e., Ac-PheProXaaIle-NH_2; Xaa = Gly, Ile). Interestingly, the physicochemical characteristics and the permeation characteristics of these tetrapeptides were similar to those of the pentapeptides. Again, as we showed in the Phe-containing pentapeptides, dramatic differences were observed between the Gly- and Ile-containing peptides (i.e., the Gly-containing tetrapeptide was approximately 130 times more able to permeate than was the Ile-containing tetrapeptide). These permeability characteristics are consistent with the observed lipophilicities of the peptides as measured by 1-octanol:HBSS partition coefficients.

Finally, it is interesting to note the differences in the metabolism characteristics of the model peptides used in these studies. All of the model peptides used in this study were acetylated at the N-terminal end and amidated at the C-terminal end in an attempt to prevent metabolism by brush border amino- and carboxypeptidases. This strategy worked very effectively for the structurally related hydrophilic peptides. In addition, we observed that those peptides (Ac-TyrProXaaIleVal-NH_2, Xaa = Gly, Ile; Ac-PheProIleIleVal-NH_2; Ac-PheProIleIle-NH_2) that exhibited low permeation across Caco-2 cell monolayers (presumably traversing the monolayer via the paracellular pathway) were metabolically stable. In contrast, those peptides that exhibited high Caco-2 cell monolayer permeation (presumably traversing the monolayer via the transcellular pathway) were extensively metabolized. Based on the results recently published by Bai (24), we assume that this metabolism occurs at the ProXaa bond and is catalyzed by prolyl endopeptidases. Bai (24) has shown that this is a cytoplasmic enzyme that is capable of catalyzing the metabolism of N-terminally acetylated neurotensin 8–13 (Ac-ArgArgProTyrIleLeu) at the ProTyr peptide bond.

In conclusion, these results with the hydrophilic peptides suggest that if the pore radii of the TJs in the Caco-2 cell monolayer are significantly larger than the molecular radii of the peptide (i.e., pore radii ≈ 12 Å; peptide radii 5–6 Å), the solution structure of the peptide can influence ite permeation. However, the effect of the solution structure of the molecule on its paracellular permeation can be overwhelmed by other physiochemical characteristics of the peptide (i.e., charge). Thus, no single physiochemical characteristic controls the paracellular permeation of peptides; instead, it is the interplay of these physicochemical characteristics that will determine their paracellular permeation characteristics. However, for hydrophobic peptides, these results suggest that solution structures (i.e., β-turns) may have a dramatic effect on the physicochemical characteristics and, thus, the membrane permeability characteristics of peptides. In addition, these results illustrate that structural changes in a peptide that lead to an increase in monolayer permeability via a change in the pathway of permeation (i.e., paracellular to transcellular) can also lead to altered pathways of metabolism.

ACKNOWLEDGMENTS

This work was supported in part by research grants from Glaxo, Inc., Costar Corp. and the United States Public Health Service (GM-51633, GM-088359). We would also like to thank Dr. Seetharama Jois for his helpful advice on the interpretation of the CD results, Dr. Martha Morton for her assistance with the NMR experiments, Dr. David J. Skanchy for his assistance with the CZE studies, and Mr. Jason Peterson, Mr. Tyler MacMillan, and Ms. Haleh Taghivi for their technical assistance with this project.

REFERENCES

1. G. M. Pauletti, S. Gangwar, G. T. Knipp, M. M. Nerurkar, F. W. Okumu, K. Tamura, T. J. Siahaan, and R. T. Borchardt. *J. Controlled Release* **41**:3–17 (1996).
2. G. M. Pauletti, S. Gangwar, T. J. Siahaan, J. Aubé, and R. T. Borchardt. *Adv. Drug Del. Rev.* (in press).
3. G. M. Pauletti, F. W. Okumu, and R. T. Borchardt. *Pharm. Res.* **14**:164–168 (1997).
4. P. S. Burton, R. A. Conradi, N. F. H. Ho, A. R. Hilgers, and R. T. Borchardt. *J. Pharm. Sci.* **85**:1336–1340 (1996).
5. G. M. Pauletti, S. Gangwar, B. Wang, and R. T. Borchardt. *Pharm. Res.* **14**:11–17 (1997).
6. G. M. Pauletti, S. Gangwar, F. W. Okumu, T. J. Siahaan, V. J. Stella, and R. T. Borchardt. *Pharm. Res.* **13**:1615–1623 (1996).
7. S. Gangwar, S. D. S. Jois, T. J. Siahaan, D. G. Vander Velde, V. J. Stella, and R. T. Borchardt. *Pharm. Res.* **13**:1657–1662 (1996).
8. S. Gangwar, G. M. Pauletti, T. J. Siahaan, V. J. Stella, and R. T. Borchardt. *J. Org. Chem.* **62**:1356–1362 (1997).
9. B. Wang, S. Gangwar, G. M. Pauletti, T. J. Siahaan, and R. T. Borchardt. *J. Org. Chem.* **62**:1363–1367 (1997).
10. F. W. Okumu, G. M. Pauletti, D. G. Vander Velde, T. J. Siahaan, and R. T. Borchardt. *Pharm. Res.* **14**:169–175 (1997).

11. H. J. Dyson, M. Rance, R. A. Houghten, R. A. Lerner, and P. Wright. *J. Mol. Biol.* **201**:161–200 (1988).
12. Y. J. Yao and S. F. Y. Li. *J. Chrom. Sci.* **32**:117–120 (1994).
13. J. Fogh, J. M. Fogh, and T. Ofreo. *J. Nat. Cancer Inst.* **59**:221–226 (1977).
14. G. T. Knipp, N. F. H. Ho, C. L. Barsuhn, and R. T. Borchardt. *J. Pharm. Sci.* **86** (1997). In press.
15. A. Perczel and M. Hollósi. in G. D. Fasman (ed.), *Circular Dichroism and the Conformational Analysis of Biomolecules*, Plenum Press, New York; 1996, pp. 285–380.
16. A. Adson, T. J. Raub, P. S. Burton, C. L. Barsuhn, A. R. Hilgers, K. L. Audus, and N. F. H. Ho. *J. Pharm. Sci.* **83**:1529–1536 (1994).
17. P. S. Burton, R. A. Conradi, and A. R. Hilgers. *Adv. Drug Del. Rev.* **7**:365–386 (1991).
18. P. Artursson and C. Magnusson. *J. Pharm. Sci.* **79**:595–600 (1990).
19. L.-S. Gan, P.-H. Hsyu, J. F. Pritchard, and D. Thakker. *Pharm. Res.* **10**:1722–1725 (1993).
20. D. Eisenberg, M. Wesson, and W. Wilcox. in G. D. Fasman (Ed.), *Prediction of Protein Structure and the Principles of Protein Conformation*, Plenum Press, New York; 1996, pp. 635–646.
21. P. S. Burton, R. A. Conradi, A. R. Hilgers, N. F. H. Ho, and L. L. Maggiora. *J. Controlled Release* **19**:87–98 (1992).
22. F. Macquaire, F. Baleux, E. Giaccobi, T. Huynh-Dinh, J.-M. Neumann, and A. Sanson. *Biochemistry* **31**:2576–2582 (1992).
23. A. Milon, T. Miyazawa, and T. Higashijima. *Biochemistry* **29**:65–75 (1990).
24. J. P. F. Bai. *Int. J. Pharm.* **112**:133–141 (1997).